Implementation of Fractional Constitutive Equations Into the Finite Element Method

Gaul, L.; Schmidt, A.
University of Stuttgart, Institute of Applied and Experimental Mechanics
Pfaffenwaldring 9, 70550 Stuttgart, Germany

ABSTRACT
The damping properties of materials, joints, and assembled structures can be modeled efficiently using fractional derivatives in the respective constitutive equations. The respective models describe the damping behavior accurately over broad ranges of time or frequency where only few material parameters are needed. They assure causality and pure dissipative behavior. Due to the non-local character of fractional derivatives the whole deformation history of the structure under consideration has to be considered in time-domain computations. This leads to increasing storage requirements and high computational costs. A new concept for an effective numerical evaluation makes use of the equivalence between the Riemann-Liouville definition of fractional derivatives and the solution of a partial differential equation (PDE). The solution of the PDE is found by applying the method of weighted residuals where the domain is split into finite elements using appropriate shape functions. This approach leads to accurate results for the calculation of fractional derivatives where the numerical effort is significantly reduced compared with alternative approaches. Finally, this method is used in conjunction with a spatial discretization method and a simple structure is calculated. The results are compared to those obtained from alternative formulations by means of accuracy, storage requirements, and computational costs.

KEYWORDS: fractional derivatives, damping, creep, constitutive equations, finite element method

1. INTRODUCTION

It is known that all structural materials show damping to some extent. When subjected to time periodic loads, a hysteresis can be observed and as a response to a Heaviside step in stress or strain, creep or stress relaxation occurs. The damping properties of some materials, such as rubbers or polymers, are quite pronounced and cannot be neglected when a structure containing these materials is modeled.
Damping models which show good adaptivity to measured material data can be obtained by introducing fractional derivatives in the respective constitutive equations. The application of fractional derivatives to viscoelasticity was studied substantially by Caputo and Mainardi [5] and is physically founded [3]. This concept results in fractional-order differential stress-strain relations, that provide good curve-fitting properties, require only few parameters, and lead to causal behavior [1, 2]. Bagley and Torvik [4] derived constraints for the material parameters of the 'fractional 3-parameter model' in order to ensure a non-negative internal work and rate of energy dissipation. Koeller [7] suggested to replace the viscous dashpots in rheological models by fractionally generalized elements which he called 'spring-pots'. The resulting constitutive relations then are consistent with thermodynamical principles [8]. An implementation of fractional constitutive equations into FE formulations is given by Padovan [10]. Parameter identifications in the time domain and in the frequency domain for the fractional 3-parameter model in conjunction with 3D FE calculations were presented by Schmidt and Gaul [11]. Enelund and Josefson [6] studied formulations of hereditary integral type in the FEM.

Since fractional derivatives are non-local operators, the actual behavior of 'fractional models' depends on the entire deformation history. Thus, in contrast to classical models, the numerical effort and the storage requirements increase with simulation time if the response of a system is computed in the time-domain. Consequently, different researchers [6, 12, 13, 14] made attempts to overcome this drawback. Two of these concepts will be discussed and compared in the following Sections.

2. NUMERICAL EVALUATION OF FRACTIONAL DERIVATIVES

In this Section, the approach made by Schmidt an Gaul [12] (concept A) will be introduced.

Using the Grünwald definition of fractional derivatives, see [9]

$$ {}_0\mathrm{D}_t^\alpha f(t) = \lim_{n\to\infty} \left(\frac{t}{n}\right)^{-\alpha} \sum_{j=0}^{n-1} A_{j+1} f_j \,, \tag{1} $$

where $f_j = f(t_\mathrm{a} - j\,t/n)$ and the Grünwald coefficients are given by

$$ A_{j+1} = \frac{\Gamma(j-\alpha)}{\Gamma(-\alpha)\Gamma(j+1)} = \frac{j-1-\alpha}{j} A_j \,. \tag{2} $$

A time-discrete approximation is obtained for a finite number n for which the expression $t/n = \Delta t$ (G1-algorithm, see [9])

$$ {}_0\mathrm{D}_t^\alpha f(t) = \Delta t^{-\alpha} \sum_{j=0}^{n-1} A_{j+1} f_j \tag{3} $$

can easily be obtained. As can be seen from Eq. (3), the numerical costs explode with the number n of time steps under consideration.

One basic idea for the reduction of the numerical effort is to reduce the computational costs by adapting the temporal resolution. Due to the fact that the Grünwald coefficients are converging towards zero for any order of derivative $\alpha > 0$ [12], events are faded out and possess a decreasing influence on the evaluation of the fractional derivative as time elapses. Using Eq. (3), the fractional derivative of a function $f(t)$ evaluated at the actual time t_a can be written as

$$ {}_0\mathrm{D}_{t_\mathrm{a}}^\alpha f(t) = {}_0\mathrm{D}_{t_\mathrm{I}}^\alpha(t_\mathrm{a}) f(t) + {}_{t_\mathrm{I}}\mathrm{D}_{t_\mathrm{a}}^\alpha(t_\mathrm{a}) f(t) \,, \tag{4} $$

where the notation ${}_a\mathrm{D}_b(t_\mathrm{a})$ shall denote the evaluation of the fractional derivative at the time t_a which may be different from the upper terminal b. By application of the G1 algorithm one obtains

$$ {}_0\mathrm{D}_{t_\mathrm{I}}^\alpha(t_\mathrm{a}) f(t) = \Delta t^{-\alpha} \sum_{j=i}^{i+k-1} A_{j+1} f_j, \qquad {}_{t_\mathrm{I}}\mathrm{D}_{t_\mathrm{a}}^\alpha(t_\mathrm{a}) f(t) = \Delta t^{-\alpha} \sum_{j=0}^{i-1} A_{j+1} f_j \,. \tag{5} $$

From Eq. (5) it is obvious that $i + k = n$ is the total number of time steps up to the actual time t_a. The first term ${}_0\mathrm{D}_{t_\mathrm{I}}^\alpha(t_\mathrm{a}) f(t)$ represents the contribution of the older part of the function's history to the fractional derivative. According to the basic idea, this interval, consisting of k time steps, will be kept fixed during further time integration and its influence on the fractional derivative will be treated separately. After n additional time steps one obtains

$$ {}_0\mathrm{D}_{t_\mathrm{I}}^\alpha(t_\mathrm{a} + n\Delta t) f(t) = \Delta t^{-\alpha} \sum_{j=i}^{i+k-1} A_{j+n+1}\, f_j \,. \tag{6} $$

Using the recursive relationship (2) yields

$$ \begin{aligned} {}_0\mathrm{D}_{t_\mathrm{I}}^\alpha(t_\mathrm{a} + n\Delta t) f(t) = \Delta t^{-\alpha} A_{i+n+1} \Bigg[1\, f_i + \frac{i+n+\alpha}{i+n+1}\, f_{i+1} + \frac{(i+n+\alpha)(i+n+1-\alpha)}{(i+n+1)(i+n+2)}\, f_{i+2} + \cdots \\ + \frac{(i+n+\alpha)(i+n+1-\alpha)\cdots(i+n+k-2-\alpha)}{(i+n+1)(i+n+2)\cdots(i+n+k-1)}\, f_{i+k-1} \Bigg] = \Delta t^{-\alpha} A_{i+n+1} T_n \,, \end{aligned} \tag{7} $$

where T_n will be called the 'transfer function'. From Eq. (7) it can be seen that all weighting factors in the square brackets are positive but smaller or equal to unity. In addition, as time elapses (n increases), they are monotonically increasing and tend to unity. In order to reduce the numerical costs, the factor T_n , which includes the contribution of k function values, will be approximated as *one* contribution to the fractional derivative. This is done by calculating the starting value T_0 according to Eq. (7) at the time t_a and the value

$$ T_\infty = f_i + f_{i+1} + f_{i+2} + \cdots + f_{i+k-1} \tag{8} $$

for $t \to \infty$. The time-dependent transfer from T_0 to T_∞ is then approximated by a test function $f(t) = 1$ such that

$$T_n \approx T_0 + \frac{T_n^{\mathbf{1}} - T_0^{\mathbf{1}}}{T_\infty^{\mathbf{1}} - T_0^{\mathbf{1}}}(T_\infty - T_0) = T_0 + w_n(T_\infty - T_0)\,, \quad w_n \in [0,\,1] \tag{9}$$

in which the upper right bold-face index $\mathbf{1}$ denotes that the respective transfer function is calculated using the test function $f(t) = 1$. The quality of the approximated transfer function is discussed in detail in [12].

For longer calculation times several intervals, each of length $k\,\Delta t$, are introduced as the number of time steps increases.

2.1 Implementation of fractional constitutive equations into the finite element method

Any general 3d fractional constitutive equation relating the stresses $\boldsymbol{\sigma}$ and strains $\boldsymbol{\varepsilon}$ can be written in the form

$$\sum_{i=1}^{n} a_i\, {}_0\mathrm{D}_t^{\alpha_i}\boldsymbol{\sigma} = \sum_{j=1}^{m} b_j\, {}_0\mathrm{D}_t^{\beta_j}\boldsymbol{\varepsilon}\,. \tag{10}$$

Using the Grünwald approximation (3) for all fractional derivatives, Eq. (10) can explicitly be solved for the actual stresses $\boldsymbol{\sigma}(\boldsymbol{t})$ which then depends on the actual strains $\boldsymbol{\varepsilon}(\boldsymbol{t})$, the stress history and the strain history (cf [10, 11]). From d'Alemberts principle, the equation of motion can be written in the form

$$\int_V \mathbf{B}^{\mathrm{T}}\,\boldsymbol{\sigma}\,\mathrm{d}V + \mathbf{M}\ddot{\mathbf{u}} = \mathbf{f} \tag{11}$$

where $\mathbf{B}$ contains the respective derivatives of the finite element shape functions, $\mathbf{M}$ is the mass matrix, $\mathbf{u}$ is the vector of the displacements, and $\mathbf{f}$ is the vector of the external forces. If one inserts the actual stresses from Eq. (10) into (11), the system can be solved by an explicit time integration scheme, such as the central difference method

$$\ddot{\mathbf{u}}(t) = \frac{\mathbf{u}(t+\Delta t) - 2\mathbf{u}(t) + \mathbf{u}(t-\Delta t)}{\Delta t^2} \tag{12}$$

For further details see e.g. [10].

3. CALCULATING A FRACTIONAL DERIVATE BY SOLVING A PARTIAL DIFFERENTIAL EQUATION

In the following, the approach published by Singh and Chatterjee [13] (concept B) is briefly summarized and extended for a fractional 3-parameter model. Then, an adaption for finite element calculations is presented.

A special partial differential equation (PDE)

$$\frac{\partial}{\partial t}u(\xi,t) + \xi^{\frac{1}{q}}u(\xi,t) = \delta(t), \quad u(\xi,0^-) = 0 \tag{13}$$

with the solution

$$u(\xi,t) = e^{-\xi^{\frac{1}{q}}t} \tag{14}$$

can be used to derive a method to calculate a fractional derivative [13]. Integration over ξ yields the transfer function $g(t)$ of the system

$$g(t) = \int_0^\infty e^{-\xi^{\frac{1}{q}}t}\mathrm{d}\xi = \frac{\Gamma(1+q)}{t^q}. \tag{15}$$

In general, the output $r(t)$ of a linear time invariant dynamical system is obtained by convolution of the transfer function $g(t)$ and the system input. By replacing the input $\delta(t)$ in (13) by $\dot{x}(t)$, one obtains

$$r(t) = g(t) * \dot{x}(t) = \int_0^t g(t-\tau)\dot{x}(\tau)\mathrm{d}\tau = \int_0^t \frac{\Gamma(1+q)}{(t-\tau)^q}\dot{x}(\tau)\mathrm{d}\tau \tag{16}$$

where $*$ denotes the convolution operator. Comparison of (16) with the well-known Riemann-Liouville definition of fractional derivatives [9] with vanishing initial conditions

$$\frac{\mathrm{d}^q}{\mathrm{d}t^q}x(t) = \frac{1}{\Gamma(1-q)}\int_0^t \frac{\dot{x}(\tau)}{(t-\tau)^q}\mathrm{d}\tau, \quad 0 \leq q < 1, \quad x(t \leq 0) = 0 \tag{17}$$

yields an alternative description of a fractional derivative

$$\frac{\mathrm{d}^q}{\mathrm{d}t^q}x(t) = \frac{1}{\Gamma(1+q)\Gamma(1-q)}r(t) = \frac{1}{\Gamma(1+q)\Gamma(1-q)}\int_0^\infty u(\xi,t)\mathrm{d}\xi \tag{18}$$

which can be specified after solving the underlying PDE

$$\frac{\partial}{\partial t}u(\xi,t) + \xi^{\frac{1}{q}}u(\xi,t) = \dot{x}(t), \quad u(\xi,0^-) = 0. \tag{19}$$

3.1 Solving the PDE using the method of weighted residuals

The PDE (19) cannot be solved exactly for general q and $\dot{x}(t)$, therefore an approximation of $u(\xi,t)$

$$u(\xi,t) \approx \sum_{i=1}^{n} a_i(t)\phi_i(\xi), \tag{20}$$

consisting of weighting functions $a_i(t)$ and shape functions $\phi_i(\xi)$, is used. Inserting (20) into (19) yields a residual

$$R(\xi,t) = \sum_{i=1}^{n}\left(\dot{a}_i(t)\phi_i(\xi) + \xi^{\frac{1}{q}}a_i(t)\phi_i(\xi)\right) - \dot{x}(t), \tag{21}$$

which is minimized using the weak form and the shape function $\phi_m(\xi)$

$$\int_0^\infty \left(\sum_{i=1}^{n}\left(\dot{a}_i(t)\phi_i(\xi) + \xi^{\frac{1}{q}}a_i(t)\phi_i(\xi)\right) - \dot{x}(t)\right)\phi_m(\xi)\mathrm{d}\xi = 0. \tag{22}$$

In order to get rid of the improper integral in (22), a transformation of ξ on the unit interval $[0,1]$ is performed by

$$\eta(\xi) = \frac{\xi}{1+\xi} \tag{23}$$

which yields

$$\int_0^1 \left(\sum_{i=1}^{n}\left(\dot{a}_i(t)\phi_i(\eta) + \left(\frac{\eta}{1-\eta}\right)^{\frac{1}{q}}a_i(t)\phi_i(\eta)\right) - \dot{x}(t)\right)\phi_m(\eta)\frac{1}{(1-\eta)^2}\mathrm{d}\eta = 0. \tag{24}$$

As we are interested to solve (24), we need to specify shape functions used to approximate $u(\eta,t)$. Choosing for example constant shape functions (see Figure 1), one obtains

$$\phi_i(\eta) = \begin{cases} 1 & p_{i-1} < \eta \leq p_i \\ 0 & \text{elsewhere} \end{cases} \quad \text{and} \quad \phi_n(\eta) = \begin{cases} \left(\frac{1-\eta}{1-p_{n-1}}\right)^{\frac{1+2q}{2q}} & p_{n-1} < \eta \leq p_n \\ 0 & \text{elsewhere} \end{cases} \quad i = 1,2,...,n-1. \tag{25}$$

In order to allow analytical integration of the matrix entries presented in the next part, we use an adaptive shape function $\phi_n(\eta)$.

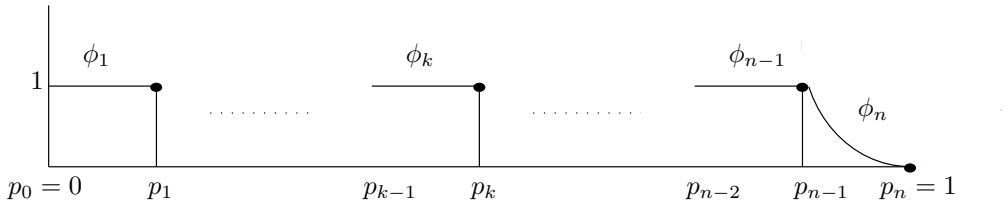

Figure 1: Constant shape functions on unit interval $\eta \in [0, 1]$

3.2 Formulation in matrix notation

Later on, we want to solve a fractional derivative in conjunction with a structural finite element discretization. Therefore, we switch to matrix notation noting that (24) can be expressed as a system of first order differential equations

$$\boldsymbol{A}\dot{\boldsymbol{a}} + \boldsymbol{B}\boldsymbol{a} = \boldsymbol{c}\dot{x}(t) \tag{26}$$

whereas

$$\boldsymbol{A}_{mi} = \int_0^1 \phi_m(\eta)\phi_i(\eta)\frac{1}{(1-\eta)^2}\mathrm{d}\eta, \tag{27}$$

$$\boldsymbol{B}_{mi} = \int_0^1 \left(\frac{\eta}{1-\eta}\right)^{\frac{1}{q}} \phi_m(\eta)\phi_i(\eta)\frac{1}{(1-\eta)^2}\mathrm{d}\eta \quad \text{and} \tag{28}$$

$$\boldsymbol{c}_m = \int_0^1 \phi_m(\eta)\frac{1}{(1-\eta)^2}\mathrm{d}\eta. \tag{29}$$

Using this notation, one can finally express a fractional derivative as

$$\frac{\mathrm{d}^q}{\mathrm{d}t^q}x(t) \approx \frac{1}{\Gamma(1+q)\Gamma(1-q)}\int_0^1 \sum_{i=1}^{n} a_i(t)\phi_i(\eta)\mathrm{d}\eta = \frac{1}{\Gamma(1+q)\Gamma(1-q)}\boldsymbol{c}^{\mathrm{T}}\boldsymbol{a} \tag{30}$$

keeping in mind from the Riemann-Liouville definition (17) that (30) is only valid if $q \in [0, 1)$.

4. A SYSTEM BASED ON FRACTIONAL 3-PARAMETER MATERIAL MODEL

Damped structures can be modeled efficiently by the use of a fractional 3-parameter material model [11] (see Figure 2) whose constitutive equation is given by

$$\sigma(t) + \frac{R}{E_1}\frac{\mathrm{d}^q}{\mathrm{d}t^q}\sigma(t) = E_0\epsilon(t) + R\frac{E_0+E_1}{E_1}\frac{\mathrm{d}^q}{\mathrm{d}t^q}\epsilon(t). \tag{31}$$

The appropriate equation of motion has the form

$$\tilde{\boldsymbol{B}}\frac{\mathrm{d}^q}{\mathrm{d}t^q}\ddot{\boldsymbol{x}} + \tilde{\boldsymbol{C}}\ddot{\boldsymbol{x}} + \tilde{\boldsymbol{D}}\dot{\boldsymbol{x}} + \tilde{\boldsymbol{E}}\frac{\mathrm{d}^q}{\mathrm{d}t^q}\boldsymbol{x} + \tilde{\boldsymbol{F}}\boldsymbol{x} = \tilde{\boldsymbol{G}}\boldsymbol{f}(t) + \tilde{\boldsymbol{H}}\frac{\mathrm{d}^q}{\mathrm{d}t^q}\boldsymbol{f}(t). \tag{32}$$

Since (30) can only be applied if $q \in [0, 1)$, the fractional derivative of $\ddot{\boldsymbol{x}}$ in (32) cannot be evaluated directly by setting

$$\frac{\mathrm{d}^q}{\mathrm{d}t^q}\ddot{\boldsymbol{x}} = \frac{\mathrm{d}^{q+2}}{\mathrm{d}t^{q+2}}\boldsymbol{x}. \tag{33}$$

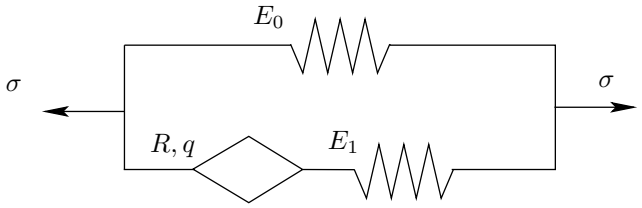

Figure 2: Fractional 3-parameter model

Instead, by introducing an additional dashpot $\tilde{R} \ll 1$ in parallel to the fractional dashpot (see Figure 3), one gets an extended fractional 3-parameter model which finally leads to a third order equation of motion of the form

$$\tilde{\boldsymbol{A}}\dddot{\boldsymbol{x}} + \tilde{\boldsymbol{B}}\frac{\mathrm{d}^q}{\mathrm{d}t^q}\ddot{\boldsymbol{x}} + \tilde{\boldsymbol{C}}\ddot{\boldsymbol{x}} + \tilde{\boldsymbol{D}}\dot{\boldsymbol{x}} + \tilde{\boldsymbol{E}}\frac{\mathrm{d}^q}{\mathrm{d}t^q}\boldsymbol{x} + \tilde{\boldsymbol{F}}\boldsymbol{x} = \tilde{\boldsymbol{G}}\boldsymbol{f}(t) + \tilde{\boldsymbol{H}}\frac{\mathrm{d}^q}{\mathrm{d}t^q}\boldsymbol{f}(t) + \tilde{\boldsymbol{I}}\dot{\boldsymbol{f}}(t) \tag{34}$$

which can easily be transformed to a set of first order differential equations.

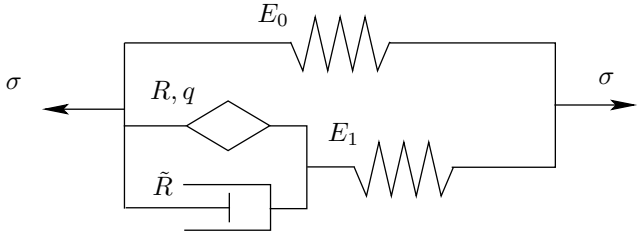

Figure 3: Extended fractional 3-parameter model

4.1 Solving a 1-DOF system

After transforming (34) into a set of first order differential equations using

$$x_1 = x, \quad x_2 = \dot{x} \quad \text{and} \quad x_3 = \ddot{x}, \tag{35}$$

on can replace each fractional derivative by (30). In the following, this process is illustrated for a 1-DOF system as shown in Figure 4. Introducing the abbreviations $E_{01} = E_0 + E_1$, the ratio of damping constants $\gamma = R/\tilde{R}$ and

$$\tilde{f} = \frac{E_1}{\tilde{R}} f(t) + \gamma \frac{\mathrm{d}^q}{\mathrm{d}t^q} f(t) + \dot{f}(t), \tag{36}$$

one finally gets $\dot{x}_1 = x_2$, $\dot{x}_2 = x_3$ and

$$\dot{x}_3 = -\gamma \frac{\mathrm{d}^q}{\mathrm{d}t^q} x_3 - \frac{E_1}{\tilde{R}} x_3 - \frac{E_{01}}{m} x_2 - \gamma \frac{E_{01}}{m} \frac{\mathrm{d}^q}{\mathrm{d}t^q} x_1 - \frac{E_0 E_1}{m\tilde{R}} x_1 + \frac{1}{m}\tilde{f}. \tag{37}$$

If the external force $f(t)$ is known in advance, then $\tilde{f}$ can be calculated after evaluating

$$\dot{\boldsymbol{a}}^{(f)} = -\boldsymbol{A}^{-1}\boldsymbol{B}\boldsymbol{a}^{(f)} + \boldsymbol{A}^{-1}\boldsymbol{c}\dot{f}(t) \tag{38}$$

whereas the index (f) in $\boldsymbol{a}^{(f)}$ denotes the application of (38) for the calculation of the external force $f(t)$. The remaining fractional derivatives in (37) can be replaced by

$$-\gamma \frac{\mathrm{d}^q}{\mathrm{d}t^q} x_3 \approx -\gamma \tilde{\Gamma}^{-1} \boldsymbol{c}^{\mathrm{T}} \boldsymbol{a}^{(x_3)} \quad \text{and} \quad -\gamma \frac{E_{01}}{m} \frac{\mathrm{d}^q}{\mathrm{d}t^q} x_1 \approx -\gamma \frac{E_{01}}{m} \tilde{\Gamma}^{-1} \boldsymbol{c}^{\mathrm{T}} \boldsymbol{a}^{(x_1)} \tag{39}$$

whereas the abbreviation $\tilde{\Gamma} = \Gamma(1+q)\Gamma(1-q)$ is used. (39) can be evaluated calculating two systems of differential equations

$$\dot{\boldsymbol{a}}^{(x_3)} = -\boldsymbol{A}^{-1}\boldsymbol{B}\boldsymbol{a}^{(x_3)} + \boldsymbol{A}^{-1}\boldsymbol{c}\dot{x}_3(t) \quad \text{and} \quad \dot{\boldsymbol{a}}^{(x_1)} = -\boldsymbol{A}^{-1}\boldsymbol{B}\boldsymbol{a}^{(x_1)} + \boldsymbol{A}^{-1}\boldsymbol{c}\dot{x}_1(t). \tag{40}$$

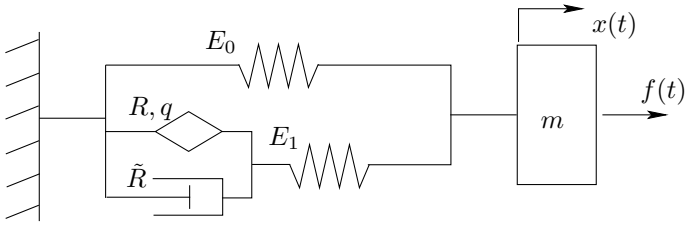

Figure 4: Mass attached to extended 3-parameter material model

Since (37) and (40) have to be calculated together, one can introduce an extended system of differential equations containing both systems

$$\begin{bmatrix} \dot{x}_1 \\ \dot{x}_2 \\ \dot{x}_3 \\ \dot{a}_1^{(x_1)} \\ \vdots \\ \dot{a}_n^{(x_1)} \\ \dot{a}_1^{(x_3)} \\ \vdots \\ \dot{a}_n^{(x_3)} \end{bmatrix} = \underbrace{\begin{bmatrix} \boldsymbol{A}_{\text{ext1}} & \boldsymbol{A}_{\text{ext2}} & \boldsymbol{A}_{\text{ext3}} \\ \boldsymbol{A}_{\text{ext4}} & \boldsymbol{A}_{\text{ext5}} & \boldsymbol{A}_{\text{ext6}} \\ \boldsymbol{A}_{\text{ext7}} & \boldsymbol{A}_{\text{ext8}} & \boldsymbol{A}_{\text{ext9}} \end{bmatrix}}_{3+2n \times 3+2n} \begin{bmatrix} x_1 \\ x_2 \\ x_3 \\ a_1^{(x_1)} \\ \vdots \\ a_n^{(x_1)} \\ a_1^{(x_3)} \\ \vdots \\ a_n^{(x_3)} \end{bmatrix} + \begin{bmatrix} 0 \\ 0 \\ \frac{1}{m}\tilde{f} \\ 0 \\ \vdots \\ 0 \\ \\ \frac{\boldsymbol{A}^{-1}\boldsymbol{c}}{m}\tilde{f} \end{bmatrix} \tag{41}$$

whereas

$$\boldsymbol{A}_{\text{ext1}} = \begin{bmatrix} 0 & 1 & 0 \\ 0 & 0 & 1 \\ -\frac{E_0 E_1}{m\tilde{R}} & -\frac{E_{01}}{m} & -\frac{E_1}{\tilde{R}} \end{bmatrix} \qquad \boldsymbol{A}_{\text{ext2}} = \begin{bmatrix} 0 & \cdots & 0 \\ 0 & \cdots & 0 \\ -\gamma\frac{E_{01}}{m}\tilde{\Gamma}^{-1}\boldsymbol{c}^{\mathrm{T}} \end{bmatrix}$$

$$\boldsymbol{A}_{\text{ext3}} = \begin{bmatrix} 0 & \cdots & 0 \\ 0 & \cdots & 0 \\ -\gamma\tilde{\Gamma}^{-1}\boldsymbol{c}^{\mathrm{T}} \end{bmatrix} \qquad \boldsymbol{A}_{\text{ext4}} = \begin{bmatrix} 0 & & 0 \\ \vdots & \boldsymbol{A}^{-1}\boldsymbol{c} & \vdots \\ 0 & & 0 \end{bmatrix} \qquad \boldsymbol{A}_{\text{ext5}} = \begin{bmatrix} -\boldsymbol{A}^{-1}\boldsymbol{B} \end{bmatrix}$$

$$\boldsymbol{A}_{\text{ext6}} = \begin{bmatrix} 0 & \cdots & 0 \\ \vdots & \ddots & \vdots \\ 0 & \cdots & 0 \end{bmatrix} \qquad \boldsymbol{A}_{\text{ext7}} = \begin{bmatrix} -\frac{E_0 E_1}{m\tilde{R}}\boldsymbol{A}^{-1}\boldsymbol{c} & -\frac{E_{01}}{m}\boldsymbol{A}^{-1}\boldsymbol{c} & -\frac{E_1}{\tilde{R}}\boldsymbol{A}^{-1}\boldsymbol{c} \end{bmatrix}$$

$$\boldsymbol{A}_{\text{ext8}} = \begin{bmatrix} -\gamma\frac{E_{01}}{m}\tilde{\Gamma}^{-1}\boldsymbol{A}^{-1}\boldsymbol{c}\boldsymbol{c}^{\mathrm{T}} \end{bmatrix} \quad \text{and} \quad \boldsymbol{A}_{\text{ext9}} = \begin{bmatrix} -\boldsymbol{A}^{-1}\boldsymbol{B} - \gamma\tilde{\Gamma}^{-1}\boldsymbol{A}^{-1}\boldsymbol{c}\boldsymbol{c}^{\mathrm{T}} \end{bmatrix}.$$

4.2 Finite element spatial discretization

In order to use the presented algorithm in conjunction with a finite element spatial discretization, it is possible to write the matrices $\tilde{\boldsymbol{A}}$ to $\tilde{\boldsymbol{I}}$ in (34) for a 2-node finite element of a rod. In this case one gets

$$\tilde{\boldsymbol{C}} = \frac{\rho A \ell}{6}\begin{bmatrix} 2 & 1 \\ 1 & 2 \end{bmatrix} \tag{42}$$

for the 'mass matrix' $\tilde{\boldsymbol{C}}$, whereas ρ denotes the material density, A describes the rod's cross section area and ℓ is the element's length. All other matrices can be determined respectively.

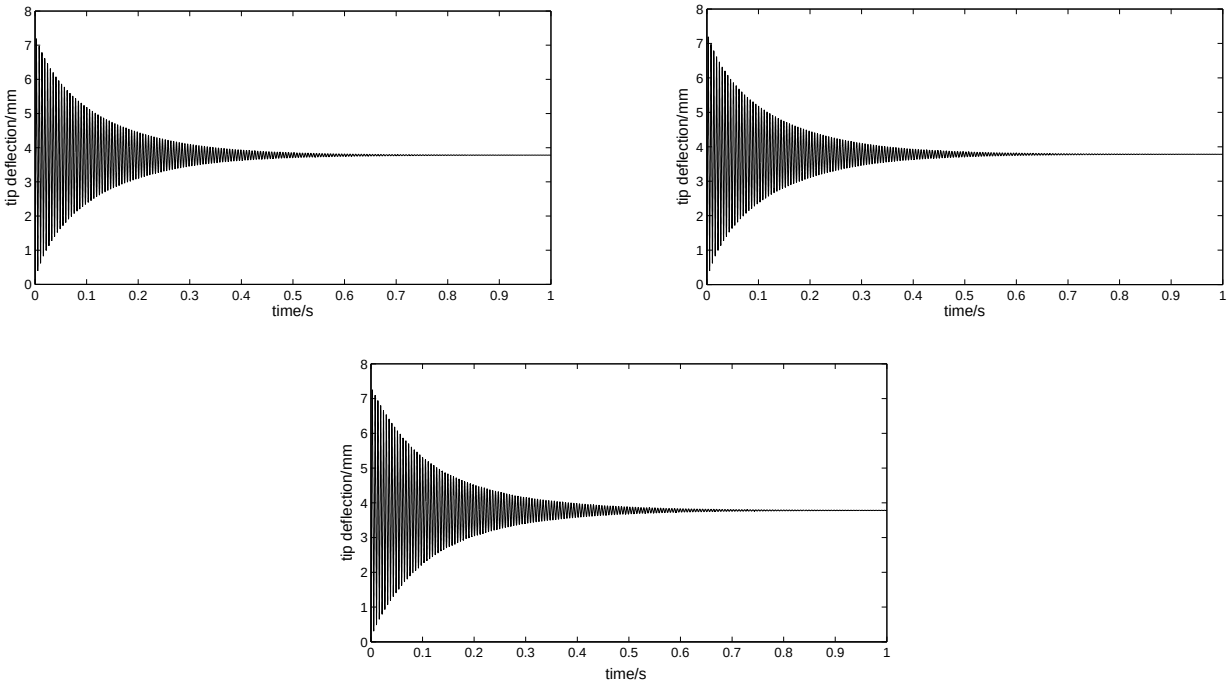

Figure 5: Decaying oscillation of the tip's free end; reference calculation (upper left), concept A (upper right) and concept B (lower)

5. EXAMPLE

As an example, a viscoelastic rod (length $\ell = 2\,\mathrm{m}$, cross section area $A = \pi(7,5\,\mathrm{mm})^2$), that is initially at rest is considered. Its left end is clamped whereas on the free end an external force $\hat{F} = 1000\,\mathrm{N}$ is acting in form of a step function in time. Thus, a free vibration is excited, overlayed by a creep process.

The rod is discretized by 30 finite elements. In order to compare the concepts A and B, given in the previous sections, the calculation is carried out using both approaches and compared with a reference calculation which is obtained using the discretized Grünwald approximation in conjunction with the complete temporal resolution as described in Section 2. The parameters used in concept A are $i = 100$, $k = 400$ whereas in concept B $n = 11$ finite elements were chosen.

The material under consideration is a thermoplastic polymer (Delrin, DuPont) and its material constants given in Table 1 are found by frequency-domain measurements [11]. The displacement of the rod's trip and its neutral position are calculated for

$E_0 = 2989.53\,\mathrm{N/mm^2}$	$E_1 = 192.92\,\mathrm{N/mm^2}$
$R = 5.276\,\mathrm{Ns^q/mm^2}$	$q = 0.5$

Table 1: Material parameters

a total simulation time of 1s, using a time step size $\Delta t = 25 \cdot 10^{-6}$s which leads to $40\,000$ time steps. The results are shown in Figure 5. A comparison in terms of the computational costs and accuracy is shown in Table 2 where the acquired time and memory resources of the reference calculation are taken to be 100%. The neutral position u_{np} is calculated from 3 subsequent extrema u_{ex} of the free vibration by

$$u_{\mathrm{np}} = \frac{u_{\mathrm{ex},1}u_{\mathrm{ex},3} - u_{\mathrm{ex},2}^2}{u_{\mathrm{ex},1} - 2u_{\mathrm{ex},2} + u_{\mathrm{ex},3}} \tag{43}$$

which gives a second-order approximation. The results are shown in Figure 6. The asymptote of the neutral position can be determined analytically by

$$\lim_{t\to\infty} u_{\mathrm{np}} = \frac{\hat{F}\ell}{E_0 A} = 3.786\,\mathrm{mm} \tag{44}$$

The scattering that can be observed in the beginning of the calculation is due to the higher harmonics which are excited by the force step function. Due to the damping they die out quite quickly. For the concept B there also seem to be some numerical reasons for the pronounced distribution.

concept	reference calculation	concept A	concept B
frequency	184.19 Hz	184.17 Hz	184.30 Hz
logarithmic decrement	4.05%	4.02%	4.22%
cpu-time	100%	3.51%	1.25%
storage	100%	52%	779%

Table 2: Comparison of accuracy, cpu-time and storage requirements of the different concepts

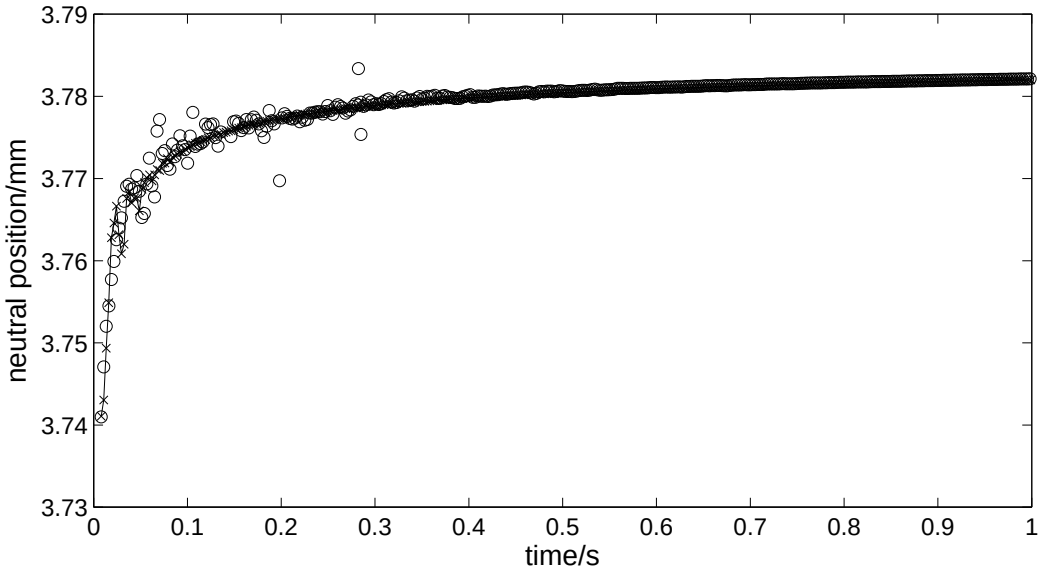

Figure 6: Calculated creep of the neutral position; reference calculation (solid), concept A (crosses), concept B (circles)

6. CONCLUSIONS

Time-domain calculations of structures whose constitutive equations include fractional derivatives lead to high computational costs, especially for large numbers of time steps. In this paper, two different concepts resulting in a drastical reduction of the numerical effort were compared with a costly reference calculation. Therefore, a new algorithm suggested by Singh and Chatterjee was extended to a fractional three-parameter model and included into a structural finite element discretization. Both concepts show very good performance concerning the reduction of calculation time. Also, the results in terms of frequency, creep process and decaying behavior are in good agreement with the reference calculation, where the algorithm by Singh and Chatterjee shows an increased scattering of the creep data. An advantage of this new algorithm is given by the fact that the time integration is unconditionally stable. Therefore, larger time steps are possible. On the other hand, the storage requirements increase drastically. In addition, more general fractional constitutive equations consisting of more than one fractional element are not straightforward to implement.

REFERENCES

[1] BAGLEY, R. L. ; TORVIK, P. J.: *A generalized derivative model for an elastomer damper*. Shock and Vibration Bulletin, 49, pp. 135–143, 1979.

[2] BAGLEY, R. L. ; TORVIK, P. J.: *Fractional calculus — a different approach to the analysis of viscoelastically damped structures*. AIAA Journal, 21(5), pp. 741–748, 1983.

[3] BAGLEY, R. L. ; TORVIK, P. J.: *A theoretical basis for the application of fractional calculus to viscoelasticity*. Journal of Rheology, 27(3), pp. 201–210, 1983.

[4] BAGLEY, R. L. ; TORVIK, P. J.: *On the fractional calculus model of viscoelastic behavior*. Journal of Rheology, 30(1), pp. 133–155, 1986.

[5] CAPUTO, M. ; MAINARDI, F.: *Linear models of dissipation in anelastic solids*. Rivista del Nuovo Cimento 1(2), pp. 161–198, 1971.

[6] ENELUND, M. ; JOSEFSON, L.: *Time-domain finite element analysis of viscoelastic structures with fractional derivatives constitutive relations*. AIAA Journal 35(10), pp. 1630–1637, 1997.

[7] KOELLER, R. C.: *Application of fractional calculus to the theory of viscoelasticity*. Journal of Applied Mechanics 51, pp. 299–307, 1984.

[8] LION, A.: *On the thermodynamics of fractional damping elements*. Continuum Mechanics and Thermodynamics 9(2), pp. 83–96, 1997.

[9] OLDHAM, K. B. ; SPANIER, J.: *The Fractional Calculus*. Academic Press, New York and London, 1974.

[10] PADOVAN, J.: *Computational algorithms for FE formulations involving fractional operators*. Computational Mechanics 2, pp. 271–287, 1987.

[11] SCHMIDT, A. ; GAUL, L.: *FE implementation of viscoelastic constitutive stress-strain relations involving fractional time derivatives*. In: *Constitutive Models for Rubber II*. A.A. Balkema Publishers, Tokyo, pp. 79–89, 2001.

[12] SCHMIDT, A. ; GAUL, L.: *On the numerical evaluation of fractional derivatives in multi-degree-of-freedom systems*. Signal Processing 86(10), pp. 2592–2601, 2006.

[13] SINGH, S. J. ; CHATTERJEE, K.: *Galerkin Projections and Finite Elements for Fractional Order Derivatives*. Nonlinear Dynamics 45(1-2), pp. 183–206, 2006.

[14] YUAN, L. ; AGRAWAL, O.: *A Numerical Scheme for Dynamic Systems Containing Fractional Derivatives*. Journal of Vibration and Acoustics 124, pp. 321–324, 2002.